Electronic supplementary information

An organophosphate 3d-4f heterometallic polyoxoniobate nanowire

Jin-Ai Fan,[†a] Hao Yu,[†a] Yu-Diao Lin,[a, b] Ming-Qiang Qi,[c] Xiang-Jian Kong,[c] Cai Sun[*a] and Shou-Tian Zheng*[*a]*

[a] *Fujian Provincial Key Laboratory of Advanced Inorganic Oxygenated Materials, College of Chemistry, Fuzhou University, Fuzhou, Fujian 350108, China*
[b]*Fujian Provincial Key Laboratory of Coastal Basin Environment, Fujian Polytechnic Normal University, Fuqing, Fujian 350300, China*
[C]*State Key Laboratory of Physical Chemistry of Solid Surface, College of Chemistry and Chemical Engineering, Xiamen University, Xiamen, 361005, China*
E-mail: csun@fzu.edu.cn; stzheng@fzu.edu.cn

†*These authors contributed equally to this work*

This file includes:

Section S1 Experiment and methods

All chemicals used for syntheses were purchased from commercial sources, and no further purifications were conducted before their usages. $K_7HNb_6O_{19}\cdot 13H_2O$ was prepared according to the literature procedure.[1] Infrared (IR) spectra (KBr pellet) were performed on an Opus Vetex 70 FTIR infrared spectrophotometer in the range of 400-4000 cm^{-1}. Powder X-ray diffraction (PXRD) patterns were recorded on a Rigaku DMAX 2500 diffractometer with Cu-*Kα* radiation (*λ* = 1.54056 Å). Thermogravimetric analysis was conducted using a Mettler Toledo TGA/SDTA 851e analyzer in an N_2-flow atmosphere with a heating rate of 10 °C/min at a temperature of 25-800 °C. The UV-vis spectra were measured on a SHIMADZU UV-2600 UV-visible spectrophotometer. Simulated XRD data was simulated by the Mercury Software with the step of 0.02° from 5° to 50° (*λ* = 1.54056 Å). Variable temperature susceptibility measurements were carried out in the temperature range of 2-300 K at a magnetic field of 0.1 T on polycrystalline samples with a Quantum Design PPMS-9T magnetometer. The experimental susceptibilities were corrected for the Pascal's constants.

Synthesis of 1: $K_7HNb_6O_{19}\cdot 13H_2O$ (0.373 g, 0.27 mmol), cobalt acetylacetonate (0.085 g, 0.24 mmol), $Dy(Ac)_3\cdot 6H_2O$ (0.156 g, 0.35 mmol), and $NaHCO_3$ (0.127 g, 1.51 mmol) were mixed in 7 mL $Na_2CO_3/NaHCO_3$ buffer solution (0.05 M, pH = 11.5) and add 80 µL EA (50% in water). to the mixture. Two minutes later, add 1 mL DMF, and after stirred 1 hour, the resulting mixture was sealed in a glass vial (20 ml) and heated at 80°C for 3 days. After cooling down, the filtrate was kept at room temperature for a week and pink block crystal of **1** suitable for X-ray diffraction experiments were obtained. Yield: ~ 30 mg (8.1 %, based on $K_7HNb_6O_{19}\cdot 13H_2O$). The pH values before and after reaction were 8.7 and 8.1, respectively. ICP, calcd (found %): Dy 8.90 (8.70), Nb 40.72 (40.66), Co 0.81 (0.86).

Synthetic discussion: Three key synthetic strategies contribute to the successful syntheses of the novel organophosphate 3d-4f heterometallic polyoxoniobate. First of them is based on the consideration of charge matching of the components in the synthesised system. Both organophosphates and PONb clusters are electronegative ligands, the introduction of relatively high-valent Ln^{3+} cations as well as transition metal ions, which act both as charge compensators

and bridges between the remaining components, opens up the possibility of composite cluster formation. The second is the judicious use of Na_2CO_3-$NaHCO_3$ buffer solution, which not only can regulate the reaction alkalinity (suitable crystallisation environments for polyoxoniobate), but also exert a slow-releasing effect for Ln^{3+} ions via coordination (with CO_3^{2-} ligand) and thus avoid the rapid precipitation of Ln^{3+} ions under basic reaction conditions. The third is our selection of transition metal ion sources, initially, we attempted the use of metal chlorides, nitrates, and acetates corresponding to Co, Ni, Cu, Fe, and Mn (both divalent and trivalent ions). Unfortunately, the introduction of these metal ions into the system in the form of acidic salts leads to their immediate hydrolysis, resulting in the formation of large amounts of flocculated material or gels. In subsequent experimental designs, we used a synthetic strategy to achieve sustained release effect by coordination with metals. We chose acetylacetonate salt as the source of 3d metal ions and a mixed solvent thermal system of DMF/buffer. The hydrolysis of 3d metal ions was synergistically inhibited by the slow release of 3d metal ions from acetylacetonate salt itself in the synthesis system as well as the coordination slow-release effect of DMF solvent. Here we interestingly found that DMF ligands the slow release of metal ions in the hydrothermal system while using its own reducing properties to reduce our introduced cobalt (III) ions to cobalt (II) ions, further inhibiting the hydrolysis of transition metal ions, and finally 3d-4f heterometallic substituted inorganic-organic hybrid PONb were successfully synthesized.

Single-crystal structure analysis: The structure of **1** was determined at 150 K under nitrogen atmosphere by single-crystal X-ray diffraction method. The apparatus is a BrukerD8 Venture diffractometer and the X-ray resource is a graphite-monochromatized Mo Kα radiation with wavelength of 0.71073 Å. The structure of **1** was solved through direct methods and refined by full-matrix least-squares refinements based on F^2 adopting the SHELXTL program package.[2] All non-H atoms were located with successive difference Fourier syntheses and refined anisotropically. The contribution of disordered solvent molecules to the overall intensity data of structures was treated using the SQUEEZE method in PLATON. Their crystallographic data can be queried with CCDC number of 2327331 at the Cambridge Crystallographic Data Centre.

Section S2 Additional Tables

Table S1 Crystal data and structure refinement for **1**

Compounds **1**	
Empirical formula	$H_{283}K_{18}Na_5Co_2C_{16}P_8Dy_8Nb_{64}O_{356}$
Formula weight	14603.5887
Crystal system	Triclinic
Space group	*P*-1
a (Å)	20.5977(14)
b (Å)	21.1986(13)
c (Å)	25.5465(17)
α (°)	66.348(2)
β (°)	88.655(2)
γ (°)	87.214(2)
V (Å^3)	10205.5(12)
Z	1
F (000)	6395
ρ_{calc} (g/cm^{-3})	2.241
Temperature (K)	150(2)
μ (mm^{-1})	3.560
Reflections collected	391554
Completeness	98.1 %
Data/restraints/parameters	36221/120/1995
GOF on F^2	1.045
Final *R* indices [I= 2σ(I)]	R_1 = 0.0479, wR_2 = 0.1329
R indices (all data)	R_1 = 0.0584, wR_2 = 0.1389

[a]$R_1 = \sum||F_o|-|F_c||/\sum|F_o|$, [b]$\omega R_2 = \{\sum\omega[(F_o)^2-(F_c)^2]^2/\sum\omega[(F_o)_2]^2\}^{1/2}$

Table S2 BVS calculations of all the Co atoms for **1**.

Atoms	Calcd for Co^{II}	Oxidation state
Co1	2.07	Co^{II}
Atoms	Calcd for Co^{III}	Oxidation state
Co1	1.76	Co^{II}

Table S3 BVS calculations of all the Dy atoms for **1**.

Atoms	Calcd for Dy^{III}	Oxidation state
Dy1	3.14	Dy^{III}
Dy2	3.21	Dy^{III}
Dy3	3.12	Dy^{III}
Dy4	3.19	Dy^{III}

Table S4 BVS calculations of all the Nb atoms for **1**.

Atoms	Calcd for Nb^{V}	Oxidation state	Atoms	Calcd forNb^{V}	Oxidation state
Nb5	5.22	Nb^{V}	Nb21	5.05	Nb^{V}
Nb6	5.12	Nb^{V}	Nb22	5.11	Nb^{V}
Nb7	5.00	Nb^{V}	Nb23	4.98	Nb^{V}
Nb8	5.13	Nb^{V}	Nb24	5.19	Nb^{V}
Nb9	5.17	Nb^{V}	Nb25	5.28	Nb^{V}
Nb10	4.99	Nb^{V}	Nb26	5.02	Nb^{V}
Nb11	5.09	Nb^{V}	Nb27	5.03	Nb^{V}
Nb12	5.02	Nb^{V}	Nb28	5.07	Nb^{V}
Nb13	5.12	Nb^{V}	Nb29	5.13	Nb^{V}
Nb14	5.05	Nb^{V}	Nb30	5.01	Nb^{V}
Nb15	5.05	Nb^{V}	Nb31	5.08	Nb^{V}
Nb16	5.01	Nb^{V}	Nb32	5.06	Nb^{V}
Nb17	5.04	Nb^{V}	Nb33	4.94	Nb^{V}
Nb18	5.05	Nb^{V}	Nb34	5.06	Nb^{V}
Nb19	4.99	Nb^{V}	Nb35	5.08	Nb^{V}
Nb20	5.02	Nb^{V}	Nb36	5.05	Nb^{V}

Table S5 The calculation of the energy barrier U_{eff} of **1**

Frequency (Hz)	Slope	U_{eff} (K)
311	0.999	0.999
511	0.876	0.876
711	0.791	0.791
911	0.729	0.729
1311	0.582	0.582
1711	0.435	0.435
2311	0.360	0.360

Section S3 Additional and characterizations structural figures

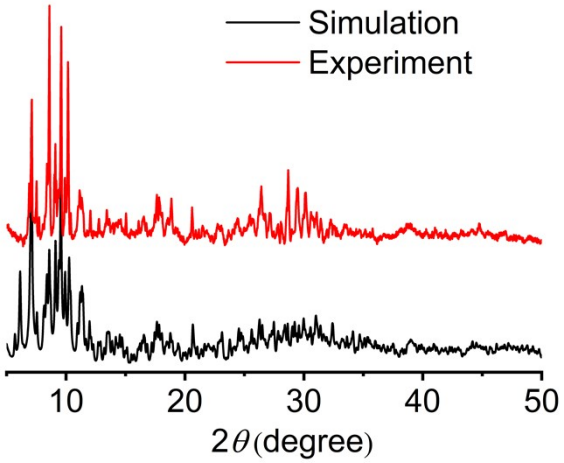

Figure S1 Experimental and simulated PXRD patterns of **1.**

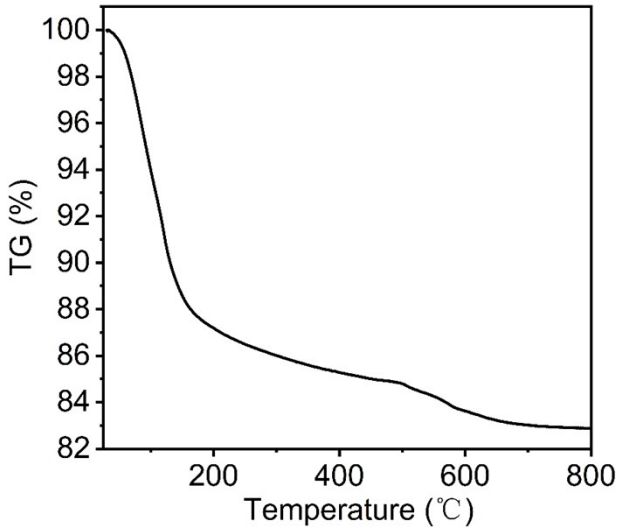

Figure S2 The TGA curve of **1**

The TGA curve was measured at a heating rate of 10 °C min^{-1} in a N_2-flow atmosphere, and the temperature range of the test was from RT to 800 °C. The compound has a continuous weight loss process in the temperature range of 25 °C to 500 °C. The first weight-loss stage should be ascribed to the loss of lattice water molecules. Based on the first weight-loss of **1**, there are about 112 lattice water molecules.

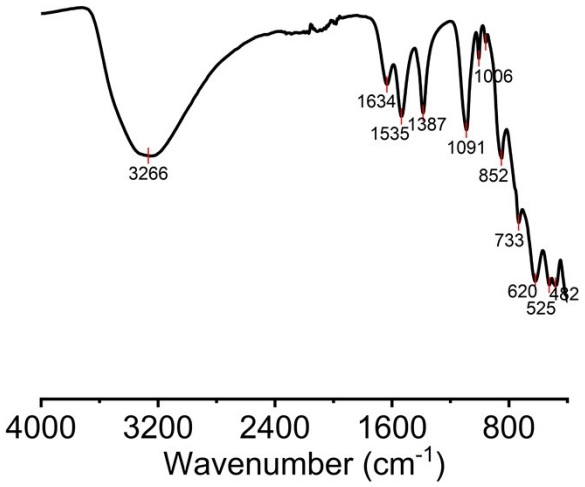

Figure S3 IR spectrum of **1**.

In the IR spectrum, the broad absorption peak at about 3266 cm^{-1} is attributed to the *v*(O-H) stretching vibration of water, and the bending vibration appear at about 1535 cm^{-1}. The *v*(C-O) stretching vibrations appear at about 1387 cm^{-1} and 1634 cm^{-1}. The *v*(P-O) stretching vibrations appear at about 1091 cm^{-1} and 1006 cm^{-1}. The peak at 852 cm^{-1} can be attributed to the stretching vibration of *v*(Nb-O_t), 733 cm^{-1}, 620 cm^{-1} and 482 cm^{-1} to the stretching vibration of *v*(Nb-O_b-Nb), and the absorption peak near 525 cm^{-1} to the stretching vibration of *v*(Dy-O).

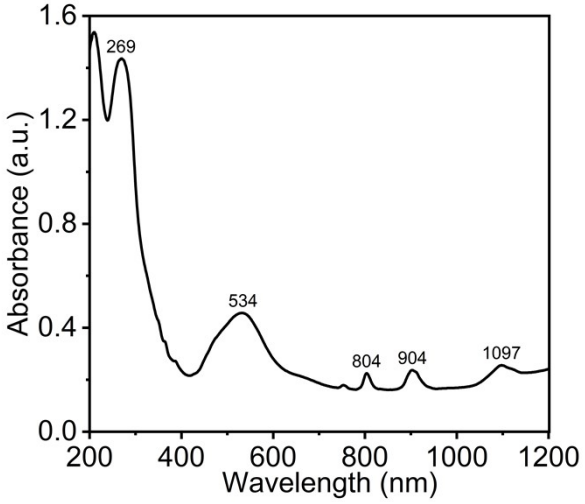

Figure S4 The solid-state diffuse reflectance UV-vis spectrum of **1**.

The UV diffuse spectrum of compound **1** is determined in the range of 200 to 1200 nm. The absorption peak in the range of 200 to 350 nm can be attributed to the charge transfer transitions from O to Nb. The broad absorption peak in the range of 400 to 600 nm can be attributed to the d-d transition of the 3d transition metal Co^{II}. The three absorption peaks in the range of 700 to1200 can be attributed to the 4f electronic energy level transition of lanthanide Dy^{III}.

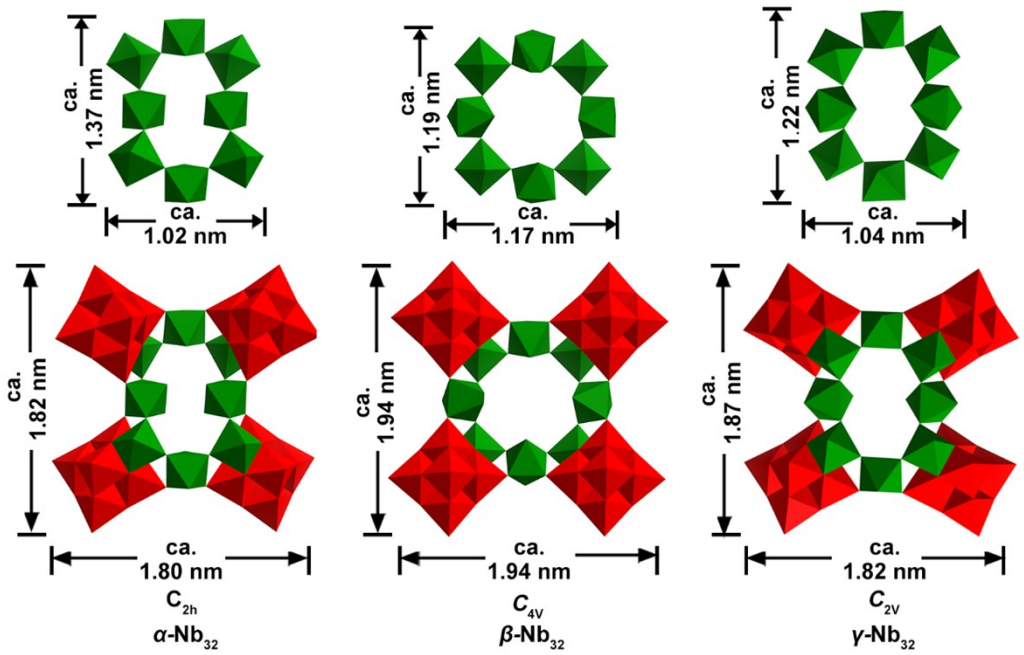

Figure S5 A structural comparison of 32-nucleairy PONb isomers: (a) *α*-Nb_{32}, (b) *β*-Nb_{32} and (c) *γ*-Nb_{32}, NbO_6 octahedra: red/green.

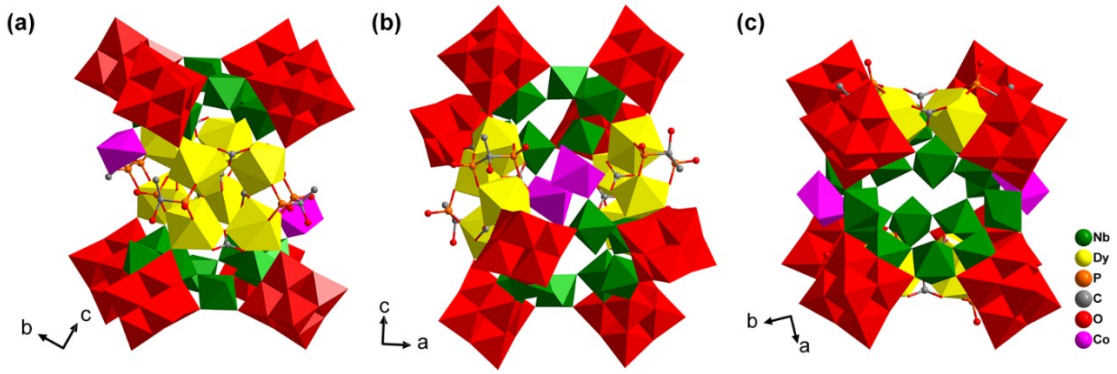

Figure S6 Diagram of different viewing directions of **1**, NbO_6 octahedra: red/green.

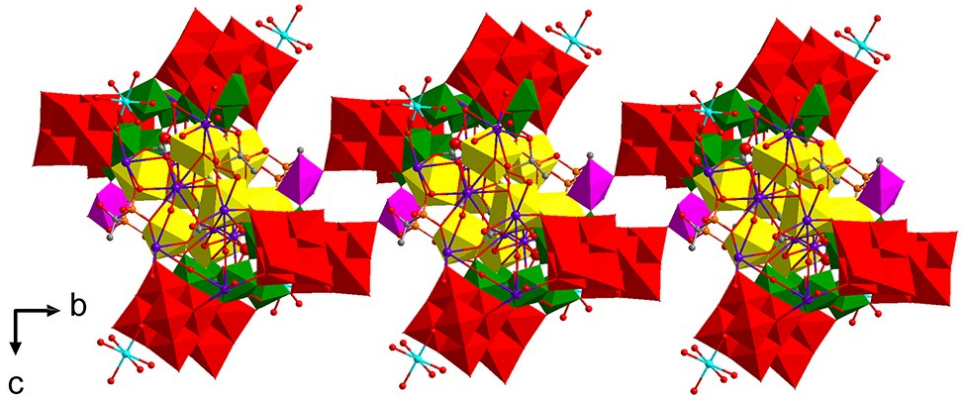

Figure S7 View of 1D chain of **1** with sodium and potassium ions. NbO_6 octahedra: red/green.

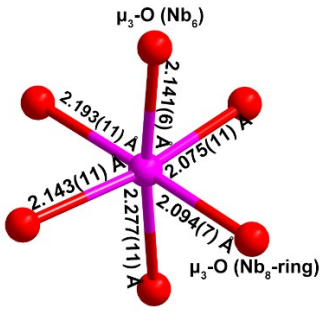

Figure S8 Coordination pattern for Co. Colour code: O, red; Co, pink.

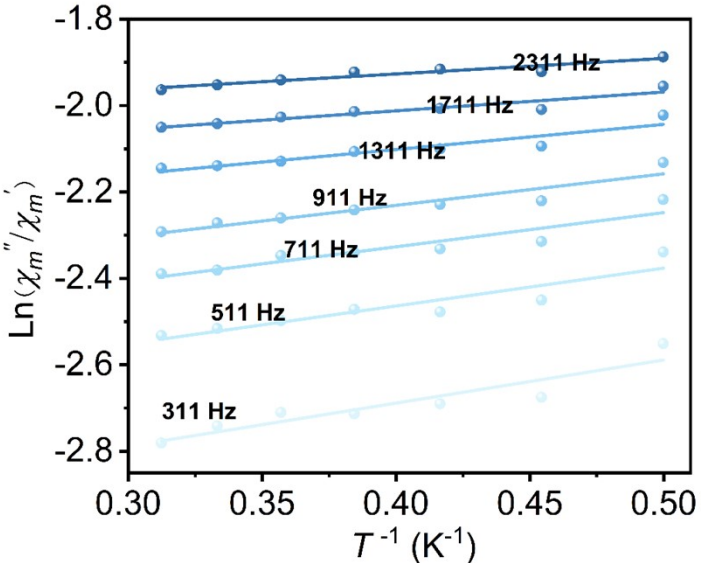

Figure S9 The calculation of the energy barrier (U_{eff}) of **1**

References

1. M. Filowitz, R. K. C. Ho, W. G. Klemperer, and W. Shum, *Inorg. Chem*., 1979, **18**, 93-103.
2. a) A. L. Spek, *J. Appl. Cryst.* 2003, **36**, 7-13; b) P. van der Sluis, A. L. Spek, *Acta Crystallogr., Sect. A*:, 1990, **46**, 194-201.